J. Hydrol. Hydromech., 71, 2023, 4, 439–448
https://doi.org/10.2478/johh-2023-0025

sciendo Journal of Hydrology and Hydromechanics Institute of Hydrology SAS

Spatial and temporal variability of saturated areas during rainfall-runoff events

Patrik Sleziak[1*], Michal Danko[1], Martin Jančo[1], Juraj Parajka[2, 3], Ladislav Holko[1]

[1] Institute of Hydrology, Slovak Academy of Sciences, Dúbravská cesta 9, 841 04 Bratislava, Slovakia.
[2] Institute of Hydraulic Engineering and Water Resources Management, TU Wien, 1040 Vienna, Austria.
[3] Centre for Water Resource Systems, TU Wien, 1040 Vienna, Austria.
[*] Corresponding author. E-mail: sleziak@uh.savba.sk

Abstract: Spatially distributed hydrological model Mike SHE was used as a diagnostic tool to provide information on possible overland flow source areas in the mountain catchment of Jalovecký Creek (area 22.2 km^2, elevation range 820–2178 m a.s.l.) during different rainfall-runoff events. Selected events represented a sequence of several smaller, consecutive events, a flash flood event and two large events caused by frontal precipitation. Simulation of hourly runoff was better for runoff events caused by heavy rainfalls of longer duration than for the flash flood or consecutive smaller runoff events. Higher soil moisture was simulated near the streamflow network and larger possibly saturated areas were located mainly in the upper parts of mountain valleys. The most pronounced increase in the areal extent of possibly saturated areas (from 6.5% to 68.6% of the catchment area) was simulated for the event with high peak discharge divided by a short rainfall interruption. Rainfall depth exceeding 100 mm caused a large increase in the potentially saturated areas that covered subsequently half of the catchment area or more. A maximum integral connectivity scale representing the average distance over which individual pixels were connected varied for the selected events between 45 and 6327 m.

Keywords: Mountain catchment; Hourly runoff simulation; Saturated area; Integrated connectivity scale.

INTRODUCTION

The fast runoff response to rainfall is a typical feature of mountain catchments (e.g. Kostka, 2009) that was attributed to retention capacity of mountain catchments (Hladný and Pacl, 1974). The high stoniness of mountain soils enhances fast water percolation through the soil profile (Hlaváčiková et al., 2016) and the shape of water outflow from the soil was found to be similar to the catchment runoff hydrograph for approximately half of the selected rainfall-runoff events (Mujtaba et al., 2020). Runoff volume during the rainfall-runoff events in mountains is primarily influenced by precipitation amount and its spatial distribution before and during the event. The influence of a catchment's wetness state before an event expressed by antecedent precipitation index (Hladný and Pacl, 1974), antecedent soil moisture (Silveira et al., 2000) or the dynamic source area concept (Myrabø, 1986) is also expected although this was not confirmed in some studies (e. g. Kostka and Holko, 2003). Areas contributing to catchment runoff vary spatially and temporally (Bracken and Croke, 2007; Hewlett and Nutter, 1970; McGuire and McDonnel, 2010; van Meerveld et al., 2015) and their variability can be investigated under the framework of the hydrological connectivity concept. Ali and Roy (2009) summarized various definitions of hydrological connectivity that were applied at both catchment and hillslopes scales. Bracken et al. (2013) stated that the most common interpretation of hydrological connectivity was related to hillslope-riparian-stream hydrological connectivity via the subsurface flow system. However, hydrological connectivity related to hydrologically relevant spatial patterns of properties (e.g. high permeability) or state variables (e.g. soil moisture) facilitating flow and transport in a hydrological system (Ali and Roy, 2009) is another definition that may be useful in the investigation of rainfall-runoff relationships. Western and Grayson (1998) documented the differences in soil moisture patterns during wet and dry periods and the appearance of connected bands of high soil moisture in drainage lines of a small catchment in southeastern Australia.

Identification of areas that become connected and contribute to streamflow during rainfall-runoff events helps shape conceptual understanding of catchment runoff formation. For instance, Ladouche et al. (2001) found for the Strengbach catchment (0.8 km^2) in Eastern France that the upper layers of saturated areas occupying only 2% of the catchment area contributed up to 30% of discharge during the initial stages of a rainfall event. However, during the final stage of the storm event, upslope/downslope areas contributed to streamflow equally. Oswald et al. (2011) found for a 71.5 ha research catchment in northwestern Ontario (Canada) that a large part of the catchment area was hydrologically disconnected from the stream during most events. Their results also showed that there was a threshold catchment storage at which larger areas contributed to streamflow. The connection of upslope areas not only leads to large changes in discharge (Detty and McGuire, 2010; van Meerveld et al., 2015) but can also cause major changes in stream water composition (e.g. Devito and Hill, 1997; Ocampo et al., 2006). While many studies of hydrological connectivity have been based on measured data in small, well instrumented experimental plots or very small research catchments, hydrological modelling can be used as a diagnostic tool in larger catchments. An example is a parsimonious spatially distributed model developed by Nippgen et al. (2015) that was used to evaluate the temporal dynamics of runoff source areas in a small, snowmelt-dominated catchment. Our study attempts to explore the employment of hydrological models as diagnostic tools for the assessment of potential runoff source areas during various types of rainfall-runoff events.

The overall objective of our study was the evaluation of the diagnostic potential of spatially distributed hydrological model Mike SHE (Mike by DHI, 2011) in investigation of runoff source

areas in a larger (22.2 km^2) mountain catchment of the Jalovecký Creek catchment in northern Slovakia. Selected rainfall-runoff events of different types during the warm period of a year (to exclude the direct influence of snowmelt) were used in the study. Specific objectives included a) evaluation of model performance in an hourly runoff simulation b) analysis of spatial and temporal variability of soil moisture during the events and c) investigation of potential hydrological connectivity during the events.

MATERIAL AND METHODS

Study area and data

The study was conducted in the mountain catchment of Jalovecký Creek (Fig. 1) in northern Slovakia. The catchment is representative of the hydrological processes in the highest part of the Carpathian Mountains. The catchment area is 22.2 km^2 and the elevations vary from 800 m a.s.l. to 2178 m a.s.l. (mean 1500 m a.s.l.). The mean slope is 30º and the catchment has predominantly southeastern to southwestern orientation. The soil cover is represented by Cambisoil, Podsol, Ranker and Lithosoil. Soil depths vary between 55–125 cm on average (Kostka and Holko, 1997). Forests dominated by spruce cover 44% of the catchment area, dwarf pine covers 31%, and alpine meadows and bare rocks cover the remaining 25% of the area.

Hourly data (precipitation, air temperature, catchment runoff and soil moisture measured at catchment mean altitude) for selected rainfall-runoff events in the warm periods of years 2014, 2015, 2017 and 2018 were used in the study. Warm periods were selected to avoid simulation of the snow cover that introduces additional uncertainties. The events are shown in Figs. 2 and 3 and represent various types of the rainfall-runoff events.

Rainfall events in summer 2014 were frequent, but did not last long. Rainfall depths during the events were approximately 40-60 mm. Several intensive rainfall bursts with an hourly rainfall depth exceeding 10 mm were recorded. The rainfall regime resulted in a greater number of relatively isolated runoff events with smaller peak discharges. Measured soil moisture increased after the first greater rainfall event at the end of June 2014 and its variability resembled that of catchment runoff. Peak flow discharges during individual events were 7–9 times greater than the discharges at the beginning of the events and runoff coefficients varied between 0.5 and 0.6. Total precipitation between 16th June 2014 and 1st September 2014 was 470.6 mm while the runoff coefficient during the same period was 0.59.

Summer 2015 was dry. Intensive rainfall that occurred on August 4 (about 16 mm in 3 hours) generated only a small runoff event (runoff coefficient 0.10), but quickly increased the soil moisture (by about 5% at the measured site shown in Fig. 2). The following, even more intensive rain on August 5 (about 45.3 mm in 2 hours) resulted in a significant runoff event with runoff coefficient 0.25 and peak flow discharge almost 17 times greater than the pre-event discharge.

Runoff events in years 2017 and 2018 had high peak flows caused by rainfall events of longer duration and quite high rainfall depths (about 24–35 hours of continuous rain before the peak flow with hourly rainfall depths of 1–10 mm). Total rainfall before the peak flow was approximately 135 mm and 178 mm in 2017 and 2018, respectively. Peak discharges were 14 (in 2017) and 29 (in 2018) times greater than the initial discharges. Total precipitation during the study periods (10th September 2017–3rd October 2017 and 16th July–9th August 2018) exceeded 200 mm and the respective runoff coefficients were 0.80 and 0.78.

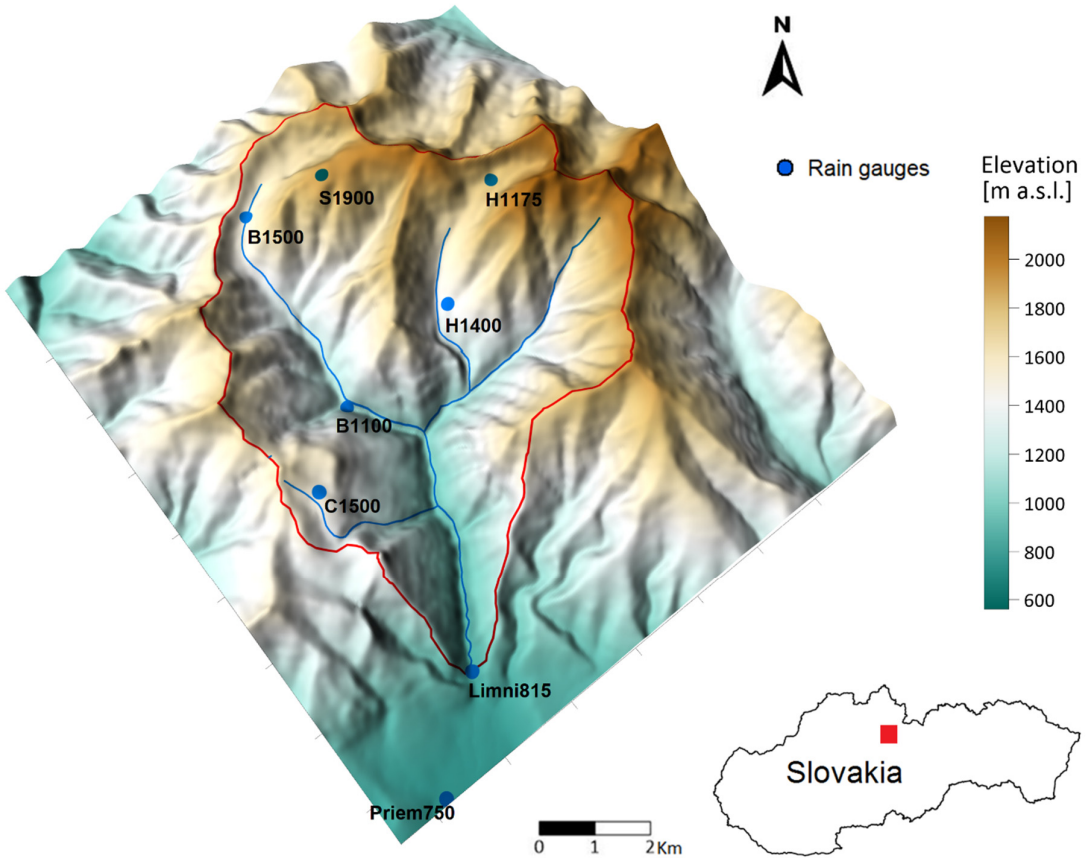

Fig. 1. Topography of the Jalovecký Creek catchment and precipitation measurement network (the blue points).

Spatially distributed hydrological modelling

Hydrological model Mike SHE (Mike by DHI, 2011) simulated catchment runoff and soil moisture in the root zone during the rainfall-runoff events at a spatial resolution of 25 m. The model was run in an hourly time step and calibrated separately for each study period (2014, 2015, 2017, 2018). Because the model was applied as a diagnostic tool, simulations in calibration and validation periods as a standard approach during the use of hydrological models as forecasting tools were not conducted. However, qualitative evaluation of the simulated outputs was conducted employing measured catchment runoff, soil moisture, runoff coefficients calculated from the total rainfall and runoff over the study periods and event water contributions estimated by the mixing formula.

Mike SHE is an established spatially distributed hydrological model that can simulate the entire land phase of the hydrological cycle depending on the components selected by the user. It can run on a daily or shorter time step. Input precipitation and air temperature in our study were based on measurements at elevations 820, 1500 and 1900 m a.s.l. Precipitation and air temperature were interpolated using the altitude gradients of 6.75%/100 m and –0.9°C/100 m for precipitation and air temperature, respectively. The annual altitude gradient in precipitation in the Jalovecký Creek catchment area in the period 2004–2022 based on measured data from elevations 700–1900 m a.s.l. varied from 37 to 81 mm/100 m. As Mike SHE uses altitude gradient in per cents to calculate the spatially distributed precipitation, these values were expressed as an 18-year average of 6.75%/100 m with a range of 3.78–9.4%/100 m. Potential evapotranspiration was calculated using the Blaney-Cridle method (Schrödter, 1985).

The model also requires geospatial input data, i.e., the raster map of digital elevation model (DEM) and vector maps of landuse and soil types. We grouped the vegetation into three groups (open area, forest and dwarf pine) and defined the leaf area index and the depth of the root zone for each zone, which we later calibrated. For the open area (grass) the depth of the root zone was calibrated in the range of 50 to 300 mm, for the forest it was between the values of 500 and 2000 mm, and for the dwarf pine it was in the range of 300 to 700 mm. Soil parameters were defined for two groups of soils One group represented forest soil for the areas covered by the forest and dwarf pine, the second the open area soil. The parameters of retention curves, hydraulic conductivity and initial soil moisture values were defined for the unsaturated zone. The surface runoff is defined by Manning's number and the height of the water at which the surface runoff occurs (detention storage). The saturated zone of the soil is defined in the model by geological units, horizontal and vertical hydraulic conductivity, external and internal boundary conditions, water level and time constant of subsurface runoff.

Runoff module parameters were calibrated by automatic optimization using the SCE method (Shuffled Complex Evolution, Duan et al., 1993). The root mean square error (RMSE) between the measured and simulated flow was used as an optimization function. The model used Richards equation to calculate the soil moisture content in the root zone.

For the calibration, we used a map resolution of 100 m, which significantly accelerated the calculation time. A total of 18 parameters were calibrated. They included two parameters for vegetation (leaf area index and depth of the root zone for the forest, dwarf pine and grass), 2 parameters for overland flow (Manning, detention storage), seven parameters for the saturated zone (vertical and horizontal hydraulic conductivity, specific yield, specific storage, lower level, drain level and time constant) and seven parameters for the unsaturated zone (saturated hydraulic conductivity, field capacity, wilting point, two empirical constants and bypass constants (maximum bypass fraction, water content for the reduced bypass flow)). Saturated soil moisture content (Theta s) was not calibrated. For the forest, it was obtained from measurements and set at a value of 0.50, and for the open area 0.48.

The Nash-Sutcliffe coefficient and regression between simulated and observed runoff were used in a quantitative evaluation of model performance. The NSE was calculated as follows:

$$NSE = 1 - \frac{\sum_{i=1}^{n} \left(Q_{sim,i} - Q_{obs,i}\right)^2}{\sum_{i=1}^{n} \left(Q_{obs,i} - \overline{Q}_{obs}\right)^2} \quad (1)$$

where $Q_{sim,i}$ and $Q_{obs,i}$ represent the simulated and observed mean daily flows on day i, and $\overline{Q}_{obs}$ is the average of the flows observed. The NSE coefficient range between –∞ and 1 (NSE = 1 indicates a perfect simulation, i.e. an absolute agreement between the observed and simulated flows).

Spatial and temporal variability of soil moisture and connectivity during selected rainfall-runoff events

The integral connectivity scale (ICS) defined in Western et al. (2001) was used as a measure of the hydrological connectivity. Connected features were understood as arbitrarily shaped bands or pathways of connected pixels having similar values of simulated soil moisture. The ICS is based on the connectivity functions representing the probability that a pixel is connected to any pixel which is separated from it by the distance *h*. The ICS is the average distance over which pixels are connected. We calculated omnidirectional ICS for the selected events and analysed its time evolution to estimate for how long the potentially saturated pixels in the catchment area were interconnected. The ICS was calculated for a threshold soil moisture of 44%. This value was chosen taking into account measured data on saturated soil conductivity and uncertainty in the Mike SHE modelling.

After evaluation of the model's performance, the rainfall-runoff events with the best hydrograph simulation were selected. Spatial variability of the simulated soil moisture during the events was analysed to evaluate the areal extent of areas with high soil moisture (i.e. potentially saturated soil) and its changes during the events. For each event, maps showing the spatial distribution of soil moisture in the catchment area at the event's beginning, in the middle of the rising hydrograph limb and at peak discharge were constructed. Field measurements (soil moisture maxima at different sites and depths in the soil) and hydrophysical characteristics of the soil samples collected in the catchment over the years indicated that the soils could be saturated at a soil moisture of approximately 49% (e.g. Hlaváčiková et al., 2014; 2017). Taking into account the uncertainty related to the Mike SHE modelling (uncertainty in inputs, model parameters, model structure, calibration approach), we considered all pixels with simulated soil moisture reaching or exceeding 44% during the events potentially saturated. This potentially saturated area was compared with the estimates from the isotopic hydrograph separations conducted in our previous works (Holko, 1995; Holko et al., 2011; 2018).

RESULTS

Hydrological model performance

Comparison of measured and simulated catchment runoff and soil moisture is shown in Figs 2 and 3. Except for the year 2014, the Nash-Sutcliffe coefficient was quite high (0.66–0.95). Better reproduction of measured catchment runoff was obtained for large runoff events caused by long rains in 2017 and 2018 (Fig. 3). Runoff simulation for a sequence of several consecutive smaller events (2014) was incorrect for several events initiated by intensive rainfall (Fig. 2). Similarly, simulation of a single runoff event caused by short rainfall of high intensity in 2015 did not produce a correct falling hydrograph limb (Fig. 2). The simulated hydrograph for this event decreased very quickly and the unrealistic delayed flow was simulated as well. This might indicate the underestimation of the subsurface flow contribution to catchment runoff during the peak flow.

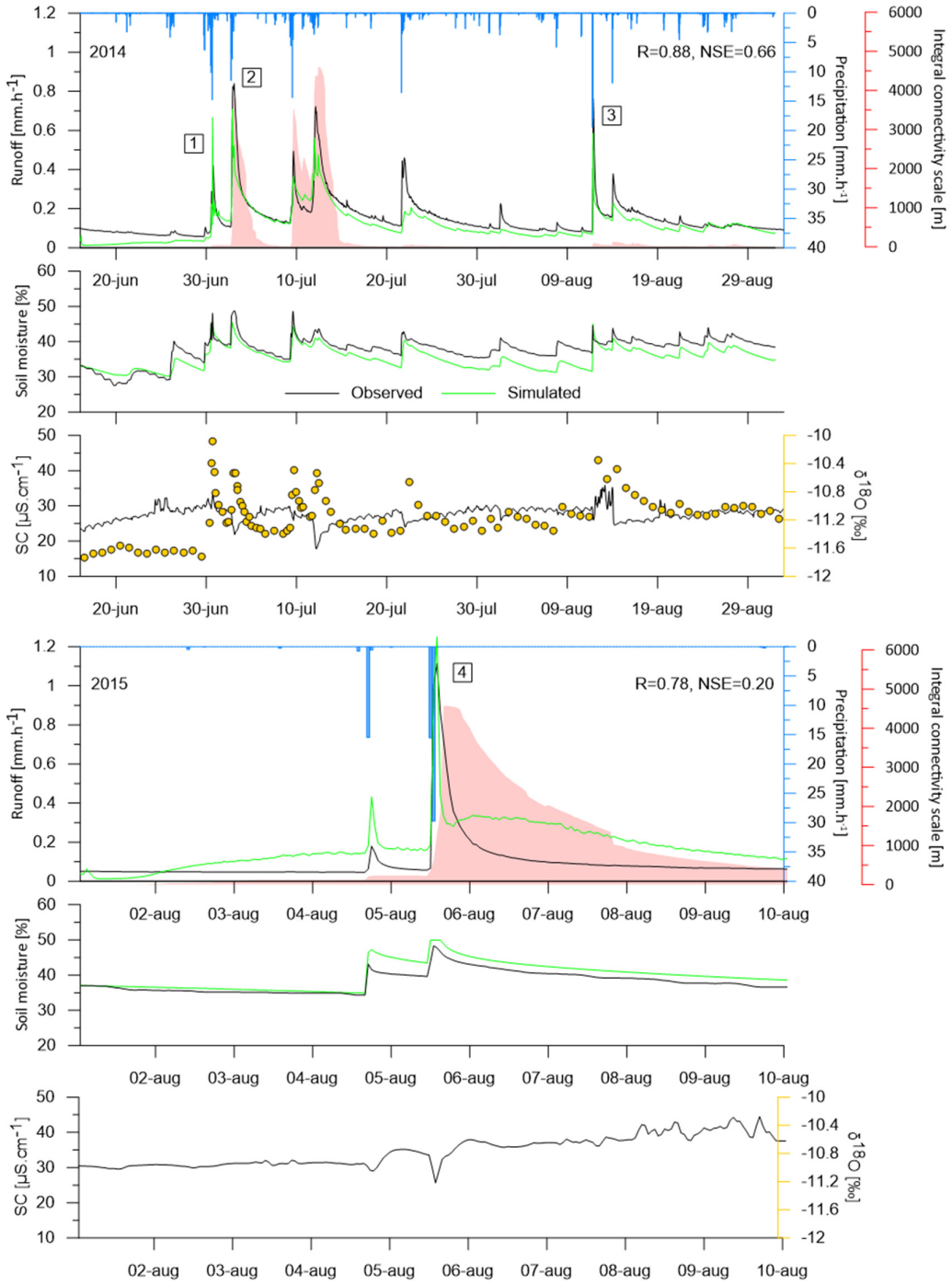

Fig. 2. Simulation of catchment runoff and soil moisture (at catchment mean altitude) in selected periods of years 2014 and 2015; electrical conductivity (EC) and $\delta^{18}O$ of Jalovecký Creek (no data for the event in August 2015), numbers in rectangles (1 to 4) denote runoff events which were selected for further evaluation. The graph also displays the calculated integral connectivity scale (ICS, red shaded area) as a measure of the presence of hydrological connectivity.

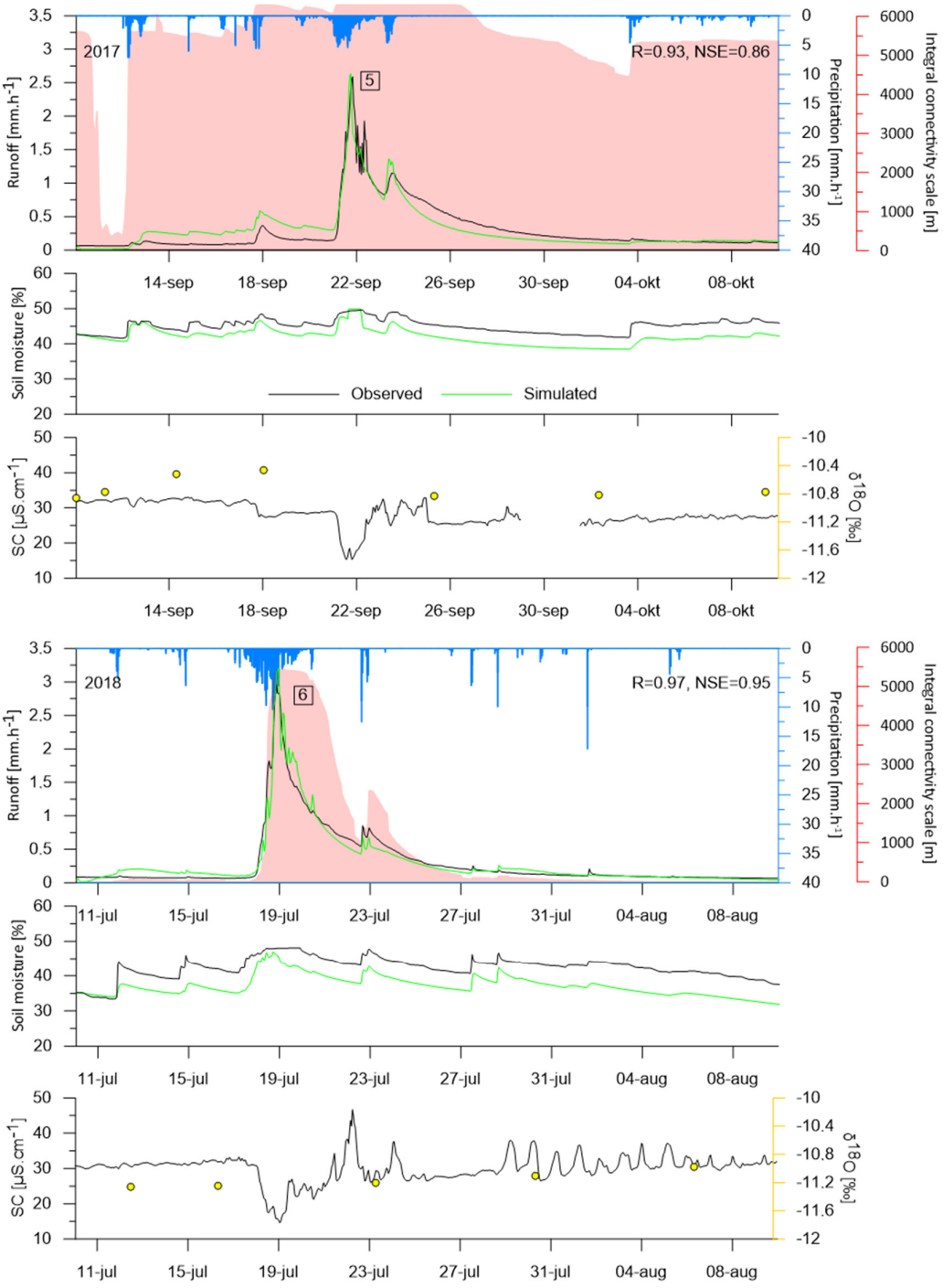

Fig. 3. Simulation of catchment runoff and soil moisture (at catchment mean altitude) in selected periods of years 2014 and 2015; electrical conductivity (EC) and $\delta^{18}O$ of Jalovecký Creek, numbers in rectangles (5 and 6) denote runoff events which were selected for further evaluation. The graph also displays the calculated integral connectivity scale (ICS, red shaded area) as a measure of the presence of hydrological connectivity.

Simulated soil moisture of the root zone reproduced measured soil moisture variability. While the measured values were underestimated for events in 2014, 2017 and 2018, for the event in 2015 they were slightly overestimated.

Qualitative evaluation of simulated outputs was based on the results of our previous studies devoted to isotopic hydrograph separations (Holko, 1995; Holko et al., 2011; 2018), comparison of the hydraulic conductivity of soils and rainfall intensities (Dóša et al., 2011; 2012) and measurement of the overland flow in the forested part of the catchment (Holko et al., 2022). These studies showed that the soil infiltration capacity was high enough to infiltrate most rainfalls, catchment runoff during the rainfall-runoff events was often dominated by the pre-event water and the overland flow in the forested part of the catchment was small, but not exceptional.

Isotopic data ($\delta^{18}O$, $\delta^{2}H$) allowing the calculation of the event water fraction in catchment runoff during the peak flow were available only for the year 2014. Event water fractions for other

years (2015, 2017, 2018) were calculated from hourly measurements of electrical conductivity (EC) in Jalovecký Creek (Figs 2 and 3). Based on our field measurements, EC of the rain water was assumed to be 10 μS cm^{-1}. Soil characteristics measured in the catchment during previous studies suggested that the infiltration excess overland flow could be generated by up to 10% of measured rainfalls. The areas generating the saturation excess overland flow could cover up to 13% of the catchment area.

The overland flow contributions to catchment runoff during peak discharges simulated by Mike SHE for the events in the year 2014 (events 1–3) were 26%, 22% and 5%. The event water contribution for events 1 and 2 were 28%–32% and 55%–64%, respectively (Holko et al., 2018). Event water contribution during event 3 based on the EC was 20%. The overland flow contributions during the peaks of runoff events 4–6 in 2015, 2017 and 2018 simulated by Mike SHE were 22%, 52%, 83%. The event water contributions calculated for the same events by the EC-based hydrograph separations were 33%, 61% and 73%, respectively. While we realize that EC is not a conservative tracer, the Mike SHE-simulated hydrograph components (overland versus subsurface flow) for events with higher peak discharge were comparable with the event/pre-event water contributions obtained from hydrograph separations within an interval of approximately ±10%.

Catchment runoff response, spatial distribution of soil moisture and connectivity during selected rainfall-runoff events

Six events (Figs 2 and 3) were selected for further investigation of potential runoff source areas and connectivity of points with high simulated soil moisture. More detailed data for these events are summarized in Table 1. Discharge before the event (Q_0) indicated that the events occurred at different catchment wetness states. This initial discharge was inversely correlated to the ratio of runoff during the rising hydrograph limb to total event runoff (Fig. 4b). However, the relationship was not very strong and Figs. 4a and 4b confirm that rainfall amount was a more important factor in influencing catchment runoff response during the events than catchment wetness state.

Spatial distribution of the soil moisture in the catchment during the rising hydrographs limbs is shown in Figs 5 and 6. Areas with high soil moisture during smaller runoff events in 2014 around the stream network expanded not only during the rising hydrographs limbs, but also between the subsequent events 1 and 2 which occurred after only a short break. The areas which could presumably be saturated according to our field and laboratory data, represented by the cells with soil moisture of 44% and higher gradually grew from approximately 0.5% of the catchment area to 26%. The wettest areas were located in the upper, comparatively flatter parts of the valleys.

The area of potentially saturated areas during the runoff event caused by the short rain outburst in 2015 was approximately 17% of the catchment. The highest soil moisture was simulated in the high parts of the catchment which could probably not cause a rapid increase of discharge at the catchment outlet (Fig. 6).

An interesting temporal variability in the spatial distribution of soil moisture was simulated for the large runoff event in 2017 caused by the long precipitation. Due to the wetter preceding period, simulated soil moisture was high already at the beginning of the event. The entire catchment should have been contributing to catchment runoff which is not realistic. Fig. 6 shows that the area with soil moisture around 50% covered a large part of the catchment during the peak flow. The model thus suggested that a greater part of the catchment contributed to runoff formation during the event in 2017. The same was indicated for the event of the same type which occurred after a longer low flow period in 2018. Areas with increased soil moisture gradually covered much of the catchment. Potentially saturated areas (soil moisture of 44% and more) increased from 6.5% of the catchment to 68.6%.

Figs. 2 and 3 show that connectivity defined by the threshold soil moisture of 44% did not develop in the catchment during the majority small runoff events with peak flow approximately below 0.4 mm h^{-1} in 2014 and 2015. On the other hand, it was at its maximum exceeding 5000 m during approximately half of the period in 2017, which seems to be too high. Peak connectivity values were usually reached after the peak flow (2014, 2015, 2018). The duration of the peak connectivity varied between 5 and 178 hours (Table 2). The time from the beginning of a runoff event (i.e. the first increase in discharge) until reaching the ICSmax varied between 3 hours for the smaller event 3 (rainfall 19 mm) and 27 hours for the large event 5 in 2017 (rainfall depth 68 mm). The results suggest that the amount of rainfall from the preceding event has a significant impact especially during larger events (events 5, 6). The total rainfall depth greater 100 mm activated a significant part of the catchment. The results indicated a longer time (from the beginning of a runoff event until the ICSmax) also during smaller consecutive events, e.g. event 1 when it was 23 hours, but the duration of the ICSmax was short (5 hours). This was probably due to the lower initial soil moisture (32%) when it took some time for the catchment to become saturated.

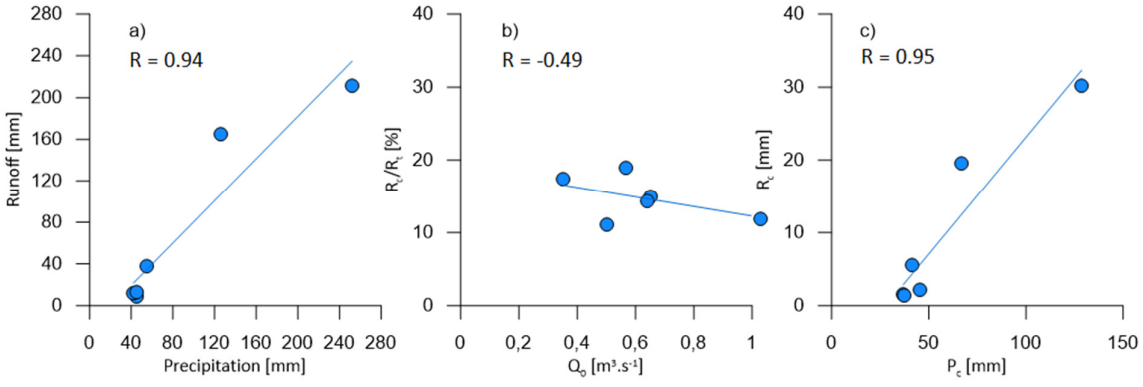

Fig. 4. Relationships between the characteristics of six selected rainfall-runoff events; a) total event precipitation and runoff, b) initial discharge Q_0 versus the ratio of runoff from event beginning to peak flow R_c to total event runoff R_t and c) precipitation (P_c) and runoff (R_c) between event beginning and peak flow; the regression lines are shown in blue.

Table 1. Characteristics of selected events; P_t and R_t are total precipitation and runoff between event beginning and end, K is runoff coefficient, R_c/R_t gives the percentage of total runoff during the event until the peak flow, Q_0 and Q_{max} are discharges at event beginning and peak; *P_t is catchment precipitation interpolated from measured values for the MikeSHE simulations.

			Measured*						Simulated MikeSHE	
Event No.	Beginning	End	P_t [mm]	R_t [mm]	K [–]	R_c/R_t [%]	Q_0 [$m^3\ s^{-1}$]	Q_{max} [$m^3\ s^{-1}$]	Q_0 [$m^3\ s^{-1}$]	Q_{max} [$m^3\ s^{-1}$]
1	6/30/2014 12:00	7/2/2014 15:00	45.2	8.5	0.19	18.9	0.357	2.600	0.358	2.251
2	7/2/2014 17:00	7/9/2014 6:00	54.5	37.4	0.69	14.9	0.651	5.182	0.825	3.223
3	8/11/2014 18:00	8/13/2014 22:00	42.3	12.1	0.29	11.2	0.500	4.699	0.424	3.610
4	8/5/2015 11:00	8/8/2015 0:00	45.5	12.8	0.28	17.5	0.414	6.877	0.995	7.703
5	9/21/2017 2:00	10/3/2017 0:00	126.5	165.2	1.31	11.9	0.873	14.660	2.082	16.258
6	7/17/2018 22:00	8/9/2018 23:00	252.15	211.82	0.84	14.3	0.418	18.240	0.945	19.458

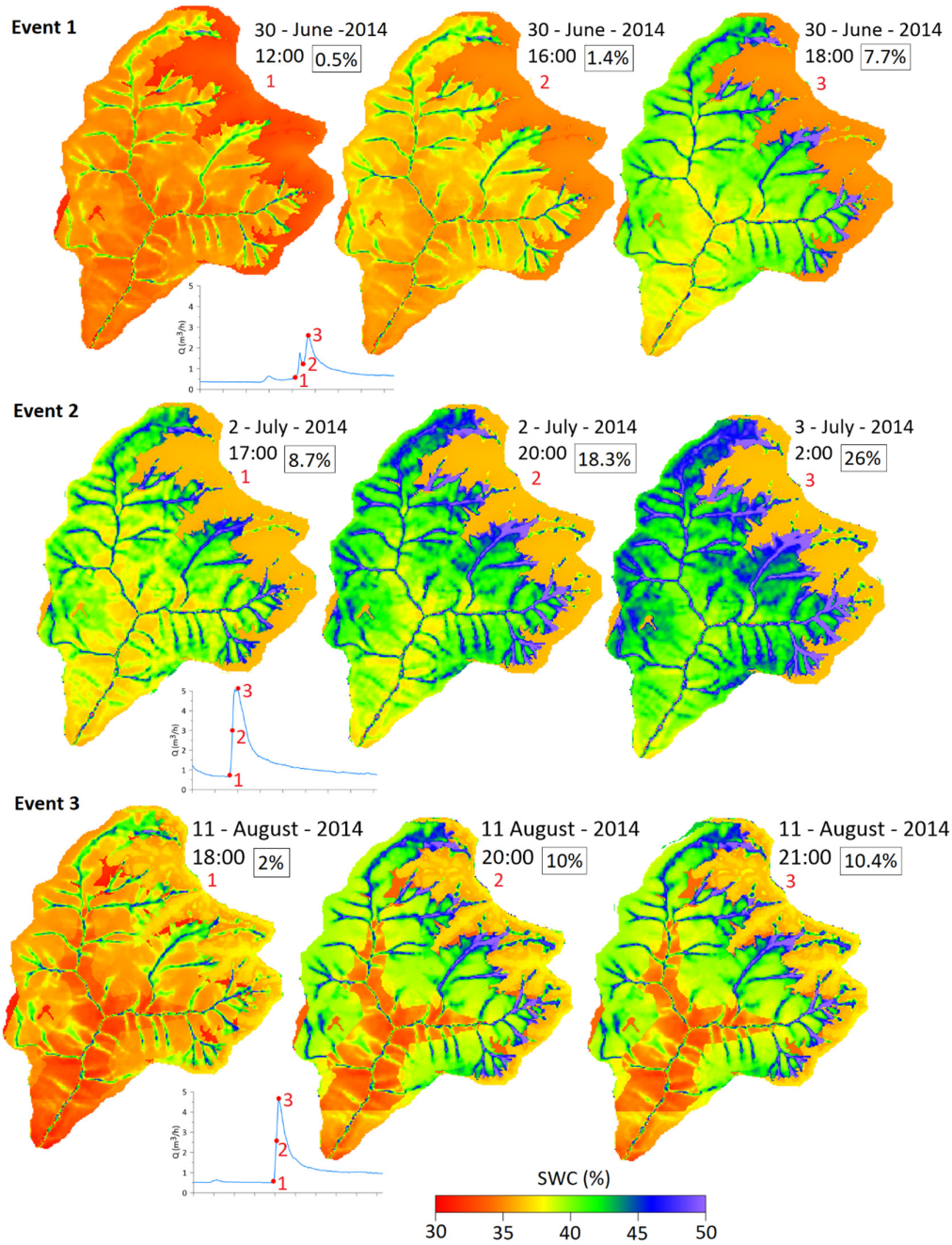

Fig. 5. Spatial distribution of soil moisture and percentage of the catchment area with potentially saturated soil (soil moisture of 44% and higher) during selected events in the year 2014.

Table 2. Characteristics of selected events; Q_{obs} is the measured discharge at catchment outlet, WC_{obs} and WC_{sim} is the observed and simulated soil moisture, respectively (at the depth of 10 cm at site C1500), P is the total rainfall depth preceding peak streamflow (5 days before the event until the event beginning), ICS is integral connectivity scale, T_1 – time from peak streamflow to ISCmax, T_2 – time from event beginning until ISCmax, T_3 – duration of ISCmax.

Event No.			Q_{obs} [m^3/s]	WC_{obs} [%]	WC_{sim} [%]	P [mm]	ICS [m]	T_1 [h]	T_2 [h]	T_3 [h]
1	Event beginning	6/30/2014 12:00	0.567	42	32	46	7	17	23	5
	ICSmax	7/1/2014 11:00	0.898	40	40		45			
2	Event beginning	7/2/2014 17:00	0.651	39	38	71	38	2	11	7
	ICSmax	7/3/2014 4:00	4.707	49	43		3814			
3	Event beginning	8/11/2014 18:00	0.500	37	32	19	3	0	3	13
	ICSmax	8/11/2014 21:00	4.699	41	44		91			
4	Event beginning	8/5/2015 11:00	0.353	40	43	18	226	3	6	6
	ICSmax	8/5/2015 17:00	3.568	45	48		4572			
5	Event beginning	9/21/2017 2:00	1.031	47	43	68	6264	11	27	118
	ICSmax	9/22/2017 5:00	8.950	50	44		6327			
6	Event beginning	7/17/2018 22:00	0.638	46	42	50	71	3	26	42
	ICSmax	7/19/2018 00:00	17.449	48	45		5447			

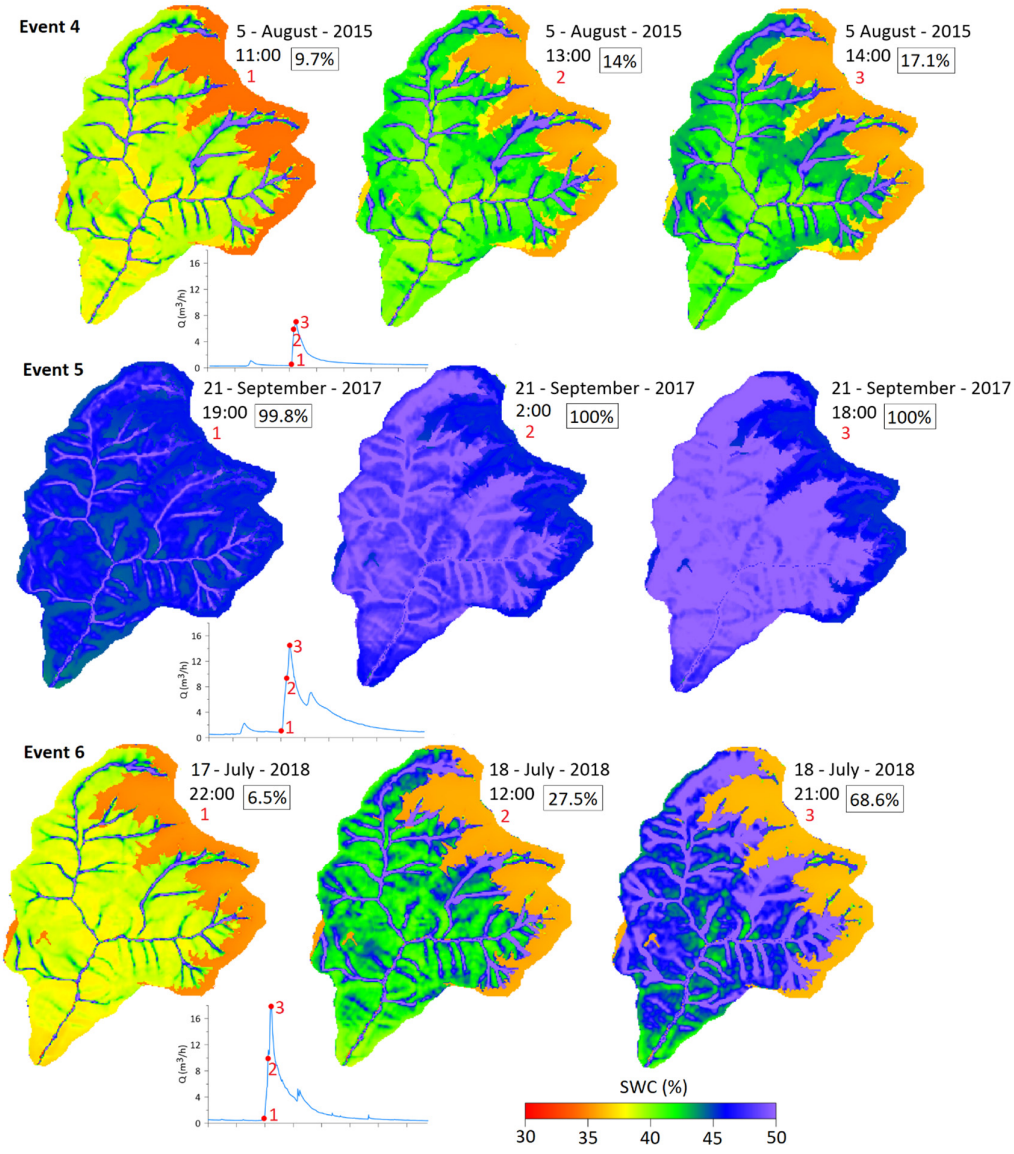

Fig. 6. Spatial distribution of soil moisture and percentage of the catchment area with potentially saturated soil (soil moisture of 44% and more) during selected events in years 2015, 2017 and 2018.

DISCUSSION

Rainfall-runoff modelling at an hourly time step provided variable results. Despite the overall good reproduction of measured runoff expressed by the Nash-Sutcliffe coefficient, closer examination of Figs 2 and 3 showed that correct simulation of peak runoff and the shapes of hydrographs at an hourly time step were sometimes challenging. This was confirmed also by the comparison of measured and simulated peak discharges for selected events (Table 1). This is similar to the results of other studies in which the peak discharges were not always simulated accurately (e.g. Bernier, 1985; Nippgen et al., 2015). It may reflect the necessity of model parameters updating during simulation of longer time series of hourly data with several rainfall-runoff events. Runoff events following short, high intensity rains, were simulated worse than those caused by moderate rains of longer duration. Such events would deserve more focused attention in our future work. The main reason for the unacceptable runoff reproduction could be related to still inadequate knowledge about catchment runoff formation during such events. This inadequate knowledge is reflected in modelling approaches that provide acceptable results for the water balance studies conducted for the longer time steps or less extreme rainfall-runoff relationships (longer moderate rainfalls with gradual catchment wetting). Focused attention on modelling of the runoff events caused by short, intensive rains (e.g. event 4 in this study) could bring new ideas about how catchments work in such situations.

Although the model was calibrated only against measured streamflow, Figs. 2 and 3 show that simulated soil moisture was generally accurate. Correlation coefficients between the simulated and measured soil moisture at a depth of 10 cm in the open area (1500 m a.s.l.) varied between 0.69 and 0.98. Similar values (0.46–0.99) were obtained also for the nearby site in the forest (1420 m a.s.l.). These results indicate that spatial patterns in simulated soil moisture could be realistic. We would like to confirm this in the future though spatially extended soil moisture measurements.

The areal extent of simulated saturated areas in the study catchment can not be validated by field measurements. However, it is interesting that in the two cases when possibly saturated areas covered more than one half of the catchment (event 6) and the entire catchment area (event 5), the preceding total rainfall depth reached 100 mm or more. The areal extent of possibly saturated areas for events with smaller preceding rainfall depths was lower than 26% regardless of peak discharge value.

Determination of possibly saturated areas and their connectivity according to simulated threshold soil moisture addresses the overland flow contribution to catchment runoff. Unlike Nippgen et al. (2015), we were not able to infer about the connectivity of the subsurface flow. Because the simulated soil moisture usually underestimated measured values, it could be assumed that the areal extent of possibly saturated areas might be greater. That would however not correspond to the estimates of saturated areas from isotopic hydrograph separation which were smaller for events 1 and 2. Nevertheless, the simulations identify areas where future measurements of soil moisture could be located to confirm their saturation during large rainfall-runoff events.

Other similar studies were usually conducted in smaller catchments with more gentle slopes connected to riparian areas and deeper soils. Our study catchment features such conditions only in the upper parts of mountain valleys while the bottom part of the catchment has steep slopes and negligible riparian areas. Kiwiet et al. (2020) reported that for the selected rainfall events in a steep small (area 20 ha) pre-Alpine headwater catchment in Switzerland, the saturated area never fell to levels below a quarter of the catchment area. We can not confirm this finding in our study catchment.

Western et al. (2001) showed that the integral connectivity scale could distinguish between the connected and disconnected soil moisture patterns in their research catchment. The small values of ICSmax values obtained in our study for events 1 and 3 (Table 2) indicate that only a small part of the catchment beyond the stream network was connected. The soil moisture threshold of 44% was probably too small for event 5. Soil moisture at the beginning of event 5 was higher than before other events (Fig. 3). Therefore, abundant rainfall that fell during the event resulted in a long period of high soil moisture. Other studies (e.g. Kiewiet et al., 2020) showed that hydrologically connected area achieved maximum two thirds of the catchment area.

The duration of connected soil moisture patterns during smaller runoff events varied (3–23 hours) while during the large events it was quite consistent (26–27 hours).

CONCLUSION

Evaluation of the performance of the spatially distributed hydrological model MIKE SHE in hourly catchment runoff simulation pointed at the need to focus on runoff events caused by short intensive rainfalls that were quite often not well simulated. Potentially saturated areas located along the stream network during smaller events expanded in the flatter parts of the mountain valleys during larger events. Field measurements should be conducted to confirm such an expansion. Quantification of the spatial extent and duration of hydrologically connected parts of the catchment during the events provided new data that is useful in thoughts concerning runoff generation in similar mountain catchments.

Acknowledgements. This study was supported by the grants from the Slovak Research and Development Agency (project APVV No. 19-0340) and the Slovak Academy of Sciences (project VEGA No. 2/0019/23).

REFERENCES

Ali, G.A., Roy, A.G., 2009. Revisiting hydrologic sampling strategies for an accurate assessment of hydrologic connectivity in humid temperate systems. Geography Compass, 3, 1, 350–374.

Bernier, B.Y., 1985. Variable source areas and storm-flow generation: An update of the concept and a simulation effort. J. Hydrol., 79, 195–213.

Bracken, L.J., Wainwright, J., Ali, G.A., Tetzlaff, D., Smith, M. W., Reaney, S. M., Roy, A. G., 2013. Concepts of hydrological connectivity: Research, approaches, pathways and future agendas. Earth Sci. Rev., 119, 17–34.

Bracken, L.J., Croke, J., 2007. The concept of hydrological connectivity and its contribution to understanding runoff dominated geomorphic systems. Hydrol. Process., 21, 2267–2274.

Detty, J.M., McGuire, K.J., 2010. Topographic controls on shallow groundwater dynamics: implications of hydrologic connectivity between hillslopes and riparian zones in a till mantled catchment. Hydrol. Process., 24, 2222–2236.

Devito, K.J., Hill, A.R., 1997. Sulphate dynamics in relation to groundwater – Surface water interactions in headwater wetlands of the southern Canadian Shield. Hydrol. Process., 11, 485–500.

Dóša, M., Holko, L., Kostka, Z., Martincová, M., 2011.

Hydraulic conductivity of the surface and maximum rainfall intensities in foothill of Jalovecký Creek catchment. Acta Hydrologica Slovaca, 12, 2, 251–258. (In Slovak.)

Dóša, M., Holko, L., Martincová, M., Danko, M., Kostka, Z., Gomboš, M., 2012. Determination of soil hydraulic conductivity in the mountain catchment by soil texture and field measurements. Acta Hydrologica Slovaca, 13, 2, 350–357. (In Slovak.)

Duan, Q.Y., Gupta, V.K, Sorooshian, S., 1993. Shuffled complex evolution approach for effective and efficient global minimization. J. Optimization Theory and Appl. 76, 3, 501–521.

Hewlett, J.D., Nutter, W.L., 1970. The varying source area of streamflow from upland basins. In: Proc. Symp. on Interdiscipinary Acpects of Watershed Management, Montana State Univ., pp. 65–83.

Hladný, J., Pacl, J., 1974. Analysis of the precipitation-runoff relationships in mountain watersheds. J. Hydrol. Hydromech., 22, 4, 346–356.

Hlaváčiková, H., Novák, V., Orfánus, T., Danko, M., Hlavčo, J., 2014. Stony soils hydrophysical characteristics. I. Hydraulic conductivities. Acta Hydrologica Slovaca, 15, 1, 24–34. (In Slovak.)

Hlaváčiková, H., Novák, V., Šimůnek, J., 2016. The effects of rock fragment shapes and positions on modeled hydraulic conductivities of stony soils. Geoderma, 281, 39–48.

Hlaváčiková, H., Holko, L. Danko, M., Kostka, Z., Hlavčo, J., 2017. Soil water regime in the mountain and foothill parts of the Jalovecký Creek catchment. In: Hydrologie malého povodí, Praha: Ústav pro hydrodynamiku AV ČR, v. v. i., pp. 35–36. ISBN 978-80-87117-15-6. (In Slovak.)

Holko, L., 1995. Stable environmental isotopes of ^{18}O and ^{2}H in hydrological research of mountainous catchment. J. Hydrol. Hydromech., 43, 4–5, 249–274.

Holko, L., Kostka, Z., Šanda, M., 2011. Assessment of frequency and areal extent of overland flow generation in a forested mountain catchment. Soil & Water Research, 6, 1, 43–53.

Holko, L., Bičárová, S., Hlavčo, J., Danko, M., Kostka, Z., 2018. Isotopic hydrograph separation in two small mountain catchments during multiple events. Cuadernos de Investigación Geográfica, 44, 2, 453–473.

Holko. L., Jančo. M., Danko, M., Sleziak, P., 2022. Influence of forest dieback on the overland flow and isotopic composition of precipitation. Acta Hydrologica Slovaca, 23, 1, 82–88.

Kiewiet, L., van Meerveld, I., Stähli, M., Seibert, J., 2020. Do stream water solute concentrations reflect when connectivity occurs in a small, pre-Alpine headwater catchment? Hydrol. Earth Syst. Sci., 24, 3381–3398.

Kostka, Z., 2009. Runoff response to rainfall even in the mountain catchment. Acta Hydrologica Slovaca, 10, 1, 113–122. (In Slovak.)

Kostka, Z., Holko, L., 1997. Soil Moisture and Runoff Generation in Small Mountain Basin. Institute of Hydrology SAS, Slovak Committee for Hydrology, Bratislava, Slovakia, 84 p.

Kostka, Z., Holko, L., 2003. Analysis of rainfall-runoff events in a mountain catchment. Technical Documents in Hydrology, No. 67, UNESCO, Paris, pp. 19–25.

Ladouche, B., Probst, A., Viville, D., Idir, S., Baqué, D., Loubet, M., Probst, J. L., and Bariac, T., 2001. Hydrograph separation using isotopic, chemical and hydrological approaches (Strengbach catchment, France). J. Hydrol., 242, 255–274.

McGuire, K.J., McDonnell, J.J., 2010. Hydrological connectivity of hillslopes and streams: Characteristic time scales and nonlinearities. Water Resour. Res., 46, W10543.

Mike by DHI, 2011. Mike SHE. An integrated hydrological modeling framework. Vol. 2. Refer. Manual, 444 p.

Mujtaba, B., Hlaváčiková, H., Danko, M., De Lima, J., Holko, L. 2020. The role of stony soils in hillslope and catchment runoff formation. J. Hydrol. Hydromech., 68, 2020, 2, 144–154.

Myrabø, S., 1986. Runoff studies in a small catchment. Nordic Hydrology, 17, 335–346.

Nash, J.E., Sutcliffe, J.V., 1970. River flow forecasting through conceptual models part I-A discussion of principles. Journal of Hydrology, 10, 3, 282–290.

Nippgen, F., McGlynn, B.L., Emanuel, R.E., 2015. The spatial and temporal evolution of contributing areas. Water Resour. Res., 51, 4550–4573.

Ocampo, C.J., Sivapalan, M., Oldham, C., 2006. Hydrological connectivity of upland-riparian zones in agricultural catchments: Implications for runoff generation and nitrate transport. J. Hydrol., 331, 643–658.

Oswald, C.J., Richardson, M.C., Branfireun, B.A., 2011. Water storage dynamics and runoff response of a boreal Shield headwater catchment. Hydrol. Process., 25, 3042–3060.

Schrödter, H., 1985. Verdunstung - Anwendungsorientierte Meßverfahren und Bestimmungsmethoden. Springer Verlag.

Silveira, L., Charbonnier, F., Genta, J.L., 2000. The antecedent soil moisture condition of the curve number procedure. Hydrol. Sci. J., 45, 1, 3-12.

van Meerveld, H.J., Seibert, J., Peters, N.E., 2015. Hillslope riparian-stream connectivity and flow directions at the Panola Mountain Research Watershed. Hydrol. Process., 29, 3556–3574.

Western, A.W., Grayson, R.B., 1998. The Tarrawarra data set: Soil moisture patterns, soil characteristics and hydrological flux measurements. Water Resour. Res., 34, 2765–2768.

Western, A., Blöschl, G., Grayson, R., 2001. Toward capturing hydrologically significant connectivity in spatial patterns. Water Resour. Res., 37, 1, 83–97.

Received 2 June 2023
Accepted 8 August 2023